



**HAL**  
open science

## **Boronic acid and diol-containing polymers: how to choose the correct couple to form “strong” hydrogels at physiological pH**

Tamiris Figueiredo, Vanina Cosenza, Yu Ogawa, Isabelle Jeacomine, Alicia Vallet, Sonia Ortega, Raphaël Michel, Johan D M Olsson, Thibaud Gerfaud, Jean-Guy Boiteau, et al.

► **To cite this version:**

Tamiris Figueiredo, Vanina Cosenza, Yu Ogawa, Isabelle Jeacomine, Alicia Vallet, et al.. Boronic acid and diol-containing polymers: how to choose the correct couple to form “strong” hydrogels at physiological pH. *Soft Matter*, 2020, 16 (15), pp.3628-3641. 10.1039/D0SM00178C . hal-03815499

**HAL Id: hal-03815499**

**<https://hal.science/hal-03815499>**

Submitted on 14 Oct 2022

**HAL** is a multi-disciplinary open access archive for the deposit and dissemination of scientific research documents, whether they are published or not. The documents may come from teaching and research institutions in France or abroad, or from public or private research centers.

L'archive ouverte pluridisciplinaire **HAL**, est destinée au dépôt et à la diffusion de documents scientifiques de niveau recherche, publiés ou non, émanant des établissements d'enseignement et de recherche français ou étrangers, des laboratoires publics ou privés.

## ARTICLE

## Boronic acid and diol-containing polymers: how to choose the correct couple to form “strong” hydrogels at physiological pH.

Tamiris Figueiredo,<sup>a</sup> Vanina Cosenza,<sup>a</sup> Yu Ogawa,<sup>a</sup> Isabelle Jeacomine,<sup>a</sup> Alicia Vallet,<sup>b</sup> Sonia Ortega,<sup>a</sup> Raphael Michel,<sup>a</sup> Johan D. M. Olsson,<sup>d</sup> Thibaud Gerfaud,<sup>c</sup> Jean-Guy Boiteau,<sup>c</sup> Jing Jing,<sup>c</sup> Craig Harris,<sup>c</sup> Rachel Auzély-Velty<sup>a\*</sup>

Received 00th January 20xx,  
Accepted 00th January 20xx

DOI: 10.1039/x0xx00000x

Dynamic covalent hydrogels crosslinked by boronate ester bonds are promising materials for biomedical applications. However, little is known about the impact of the crosslink structure on the mechanical behaviour of the resulting network. Herein, we provide a mechanistic study on boronate ester crosslinking upon mixing hyaluronic acid (HA) backbones modified, on the one hand, with two different arylboronic acids, and on the other hand, with three different saccharide units. Combining rheology, NMR and computational analysis, we demonstrate that carefully selecting the arylboronic-polyol couple allows for tuning the thermodynamics and molecular exchange kinetics of the boronate ester bond, thereby controlling the rheological properties of the gel. In particular, we report the formation of “strong” gels (i.e. featuring slow relaxation dynamics) through the formation of original complex structures (tridentate or bidentate complexes). These findings offer new perspectives for the rational design of hydrogel scaffolds with tailored mechanical response.

### Introduction

Injectable hydrogels that are capable of autonomous healing upon damage have recently drawn great attention in the fields of tissue engineering and regenerative medicine for minimally invasive delivery of cells and in the filling of irregular defects.<sup>1,2</sup> These hydrogels possess adaptable linkages that can be broken and re-formed in a reversible manner without external triggers. This feature is conducive to the homogeneous entrapment of cells *ex vivo* under physiological conditions. The mechanisms to form adaptable linkages include physical associations (hydrogen bonding, ionic, hydrophobic or host-guest interactions) and dynamic covalent chemistry.<sup>1-3</sup> Compared to physical associations, dynamic covalent reactions usually have slower bond cleavage kinetics.<sup>2,4</sup> Consequently, hydrogels based on dynamic covalent chemistry can self-repair much like physically crosslinked networks while being more stable.

As one of the dynamic covalent bonds, the boronate ester linkage has been used by several groups in an attempt to prepare autonomous self-healing hydrogel networks.<sup>5-16</sup> Such networks have emerged as promising dynamic biomedical materials as their formation occurs in aqueous solution under mild conditions and requires no catalyst.<sup>17</sup> These networks are

generally obtained by combining a polymer modified with classical phenylboronic acid (PBA), or substituted PBA derivatives, and a polymer bearing diol-containing molecules. Such systems have been obtained not only at alkaline pH (pH > 8),<sup>6,7,10,11,13</sup> but also at physiological pH (pH = 7.4),<sup>5,8,9,12,14-16</sup> depending on the chosen arylboronic acid/diol couple. At physiological pH, variations in the structure of boronic acids or diol-containing molecules not only affects the network modulus but also significantly alters the relaxation behaviour of the materials. In fact, two types of relaxation behaviour of boronate ester-crosslinked networks can be distinguished in the literature: slowly relaxing systems, i.e. exhibiting a gel-like behaviour (storage modulus ( $G'$ ) > loss modulus ( $G''$ )) within the whole range of frequencies covered), and fast relaxing networks, i.e. displaying a viscoelastic behaviour (crossover of  $G'$  and  $G''$  seen within the tested frequencies). The relationship between the nature of the couple boronic acid/diol and the network rheological behaviour still remains to be clarified. Some work suggested a possible link between the  $pK_a$  of the phenylboronic acid derivative and the rheological properties.<sup>16</sup> This relies on the fact that a pH higher than the  $pK_a$  of the PBA derivative is, in theory, required to facilitate binding of boronic acid to the diol moieties.<sup>18</sup> In this regard, phenylboronic acid derivatives possessing a  $pK_a$  near 7 have been regarded as attractive candidates to construct hydrogel networks at physiological pH.<sup>8,9,14,16</sup> Nevertheless, hydrogels networks with slow dynamics have been obtained at physiological pH via boronate ester formation between polymers modified with classical PBA (~ 8.8)<sup>18</sup> and polymers containing salicylhydroxamic acid moieties<sup>12</sup> or some sugar derivatives.<sup>15,19</sup> In particular, we previously obtained slowly relaxing self-healing hydrogels based on hyaluronic acid at physiological pH,

<sup>a</sup> Univ. Grenoble Alpes, Centre de Recherches sur les Macromolécules Végétales (CERMAV)-CNRS, 601, rue de la Chimie, BP 53, 38041 Grenoble Cedex 9 (France).

<sup>b</sup> Univ. Grenoble Alpes, CEA, CNRS, Institut de Biologie Structurale, 71 avenue des Martyrs, 38044 Grenoble Cedex 9 (France)

<sup>c</sup> Galderma/Nestlé Skin Health R&D, 2400 Route de Colles, 06410 Biot (France)

<sup>d</sup> Galderma/Nestlé Skin Health R&D, Seminariegatan 21, SE-752 28 Uppsala (Sweden)

Electronic Supplementary Information (ESI) available: [details of any supplementary information available should be included here]. See DOI: 10.1039/x0xx00000x

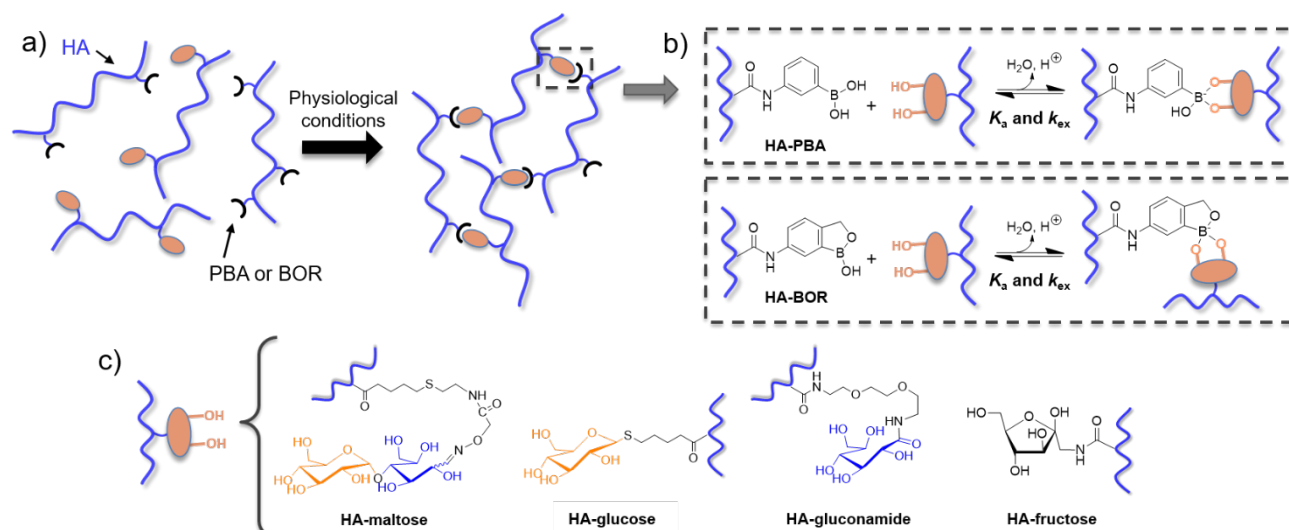


**Figure 1:** (a) Dynamic covalent hyaluronic acid hydrogels crosslinked via tunable dynamic boronate ester bonds. (b) Mechanism of boronate ester bond formation according to literature. (c) HA-saccharide derivatives investigated as partners of HA-PBA and HA-BOR to form hydrogel networks.

via boronate ester bonds between 3-aminophenylboronic acid and a maltose derivative containing a ring-opened glucose unit or fructose.<sup>15, 20</sup> On the other hand, fast relaxing networks can be also formed from polymers containing benzoboroxole (BOR)<sup>9, 21, 22</sup> despite its relatively high Lewis acidity ( $pK_a \sim 7.3$ )<sup>23, 24</sup> compared to PBA.

All these results indicate that the properties of the arylboronic acid/diol couple impact greatly the dynamics of the boronate ester bond thereby influencing the macroscopic mechanical properties of the resulting hydrogel networks. Moreover, the rheological characteristics of boronate ester crosslinks are not only related to the thermodynamics but also to their molecular exchange kinetics.<sup>14</sup> In this regard, Cromwell *et al.* recently demonstrated that the transesterification kinetics in networks based on a diol-containing polycyclooctene polymer cross-linked by telechelic diboronate ester crosslinkers is the primary determinant of the relaxation properties of these bulk solid materials.<sup>25</sup> These results are in line with the concept of "strong means slow" introduced in 2005 by Yount *et al.* in their study on supramolecular networks based on metal-ligand interactions.<sup>26</sup> These authors showed that it is the exchange kinetics of molecular crosslinks, much more than their thermodynamics, that are quantitatively responsible for the bulk viscoelastic properties of the network.<sup>26, 27</sup>

Despite the growing interest in self-healing hydrogels based on boronate esters, the relationship between the properties of the crosslinks and the mechanical behaviour of the networks, while being indispensable for their applicability, has been very little studied.<sup>14, 16</sup> Herein we address this question by investigating hyaluronic acid (HA) hydrogels crosslinked with boronate ester bonds. As one of the main components of soft tissues in the body, HA is an attractive polysaccharide building block for engineering hydrogels for cell and tissue engineering.<sup>28, 29</sup> More specifically, we investigate the relation between the molecular structure of sugar derivatives grafted on HA and their reactivity towards PBA or BOR grafted on other HA chains. Herein, BOR was selected in addition to PBA as the binding site for

carbohydrate moieties grafted on HA because of its capability to bind saccharides at physiological pH, and especially carbohydrates locked in their pyranose form for which PBA has virtually no affinity.<sup>30</sup> Thus, our investigation focused on the formation of networks from HA derivatives modified with single glucose units locked in the pyranose form (referred to as HA-glucose) or in the ring-opened form (referred to as HA-gluconamide), in comparison to HA modified with the maltose derivative (Figure 1). Moreover, taking into account the higher affinity of boronic acids towards D-fructose over D-glucose,<sup>31</sup> we also selected fructose as the binding site for PBA and BOR. The relative influence of the exchange kinetics and thermodynamics of the molecular crosslinks on the network mechanical properties was studied for each boronic acid-diol pair, both free and grafted to HA (Figure 1). In addition, NMR and computational analyses were used to provide a comprehensive picture, from a structural perspective, of the binding mode of PBA and BOR to the different saccharide derivatives.

## Experimental section

### Materials

Sodium hyaluronate (HA) possessing a weight average molar mass ( $M_w$ ) of 100 kg/mol was supplied by Lifecore Biomedical (USA). The molar mass distribution and the weight-average molar mass of this sample were determined by size exclusion chromatography using a Waters GPC Alliance chromatograph (USA) equipped with a differential refractometer and a light scattering detector (MALLS) from Wyatt (USA); the solution was injected at a concentration of  $1 \times 10^{-3}$  g/mL in 0.1 M  $\text{NaNO}_3$ , at a flow rate of 0.5 mL/min and at a column temperature of 30 °C. The dispersity ( $\mathcal{D}$ ) of the sample is  $M_w/M_n \approx 1.5$ -2. The overlap concentration  $C^*$  for this HA sample in buffer at 25 °C is around 3 g/L. This value was derived from the intrinsic viscosity assuming that  $C^*[\eta]$  is about unity.<sup>32</sup> HA samples with lower  $M_w$  (5 or 10 kg/mol), purchased from the same supplier, were used

to synthesize HA derivatives for NMR studies (thermodynamics, kinetics and elucidation of the structure of boronic acid complexes). This low  $M_w$  HA sample was used to circumvent limitations due to the high viscosity of concentrated solutions of high  $M_w$  HA. 5-amino-2-(hydroxymethyl)phenylboronic acid hydrochloride (ABOR, 6-aminobenzoboroxole) and Boc-1-amino-3,6-dioxo-8-octanamine (Boc-DOOA) were purchased from Combi-Blocks and Iris Biotech, respectively. 1-Amino-1-deoxy-D-fructose hydrochloride (fructosamine) and D-gluconolactone were supplied by Carbosynth. 3-Aminophenylboronic acid hemisulfate salt (APBA), 4-(4,6-dimethoxy-1,3,5-triazin-2-yl)-4-methylmorpholinium chloride (DMTMM), D-maltose, 1-thio- $\beta$ -D-glucose sodium salt (thioglucose), 4-pentenoic anhydride, O-(carboxymethyl)hydroxylamine hemihydrochloride, cystamine dihydrochloride, *N,N'*-diisopropylcarbodiimide (DIC), 1-hydroxybenzotriazole (HOBT), tris(2-carboxyethyl)phosphine hydrochloride (TCEP), trifluoroacetic acid (TFA), picrylsulfonic acid solution (TNBS), 4-(2-hydroxyethyl)piperazine-1-ethanesulfonic acid (HEPES), phosphate buffered saline (PBS) and other chemicals were purchased from Sigma-Aldrich-Fluka and were used without further purification. A  $^{13}\text{C}$  labelled maltose (maltose- $^{13}\text{C}_{12}$  monohydrate) was supplied by Cambridge Isotope Laboratories and a  $^{13}\text{C}$  labelled D-fructose was purchased from Carbosynth.

## Methods

**Synthesis.** All synthetic routes for the modification of HA are described in details in the Supplementary Information.

**NMR spectroscopy.**  $^1\text{H}$ ,  $^{13}\text{C}$  and 2-D INADEQUATE NMR spectra were recorded at 25 °C or 80 °C using a Bruker AVANCE III HD spectrometer operating at 400.13 MHz ( $^1\text{H}$ ) and at 100.61 MHz ( $^{13}\text{C}$ ).  $^1\text{H}$  NMR spectra were recorded by applying a 90° tip angle for the excitation pulse, and a 10 s recycle delay for accurate integration of the proton signals.  $^{13}\text{C}$  NMR spectra were recorded by applying a 90° tip angle for the excitation pulse and a 2 s recycle delay. 2-D INADEQUATE experiments were performed using the pulse sequence inadphsp given by Bruker. For each experiment, 256 transients were acquired for each of the 128 increments in F1. The recycle delay was set to 3 s. The spectral width was set to 20161 Hz (number of data points = 8192). The data were processed with shifted sine bell weighting and zero filling to form a 8192 x 1024 matrix prior to Fourier transform.  $^{13}\text{C}$ -edited HSQC experiments using the HA derivative modified with  $^{13}\text{C}$  labelled maltose were recorded on a Bruker AVANCE III HD operating at 950.23 MHz ( $^1\text{H}$ ) and at 238.94 MHz ( $^{13}\text{C}$ ) equipped with a cryogenic probe. Deuterium oxide ( $\text{D}_2\text{O}$ ) was obtained from Euriso-top (Saint-Aubin, France). Chemical shifts ( $\delta$  in ppm) are given relative to external tetramethylsilane (TMS = 0 ppm) and calibration was performed using the signal of the residual protons of the solvent as a secondary reference. All NMR spectra were analysed with Topspin 3.1 (or 3.5) software from Bruker AXS.

**Rheology.** Oscillatory shear experiments were performed with a cone-plate rheometer (AR2000EX from TA Instruments). All the dynamic rheological data were checked as a function of strain amplitude to ensure that the measurements were

performed in the linear viscoelastic region. No frequency data beyond 10 Hz are presented because inertial artefacts (raw phase angle > 150°) were observed at frequencies higher than 10 Hz.<sup>33, 34</sup> The cone used for viscoelastic samples has a diameter of 2 cm and an angle of 4°, whereas viscous solutions were analysed using a cone of 6 cm of diameter and an angle of 1°. To prevent water evaporation, the measuring system was surrounded with a low-viscosity silicon oil (50 mPa.s) carefully added to the edges of the cone.

**Determination of  $K_a$  by ITC.** Calorimetric titration experiments were carried out on a Microcal VP-ITC titration microcalorimeter (Northampton, U.S.A.). All titrations were performed using solutions of APBA (ABOR) and free saccharides (D-fructose, maltose-COOH and gluconamide) solubilized in 0.01 M PBS, with pH adjusted to 7.4 ( $\pm 0.1$ ) using a pH-meter, by carefully adding 1 M NaOH when necessary. The reaction cell ( $V = 1.4478$  mL) contained a solution of “molecule 2” (Table S1). A series of 28 injections of 5 or 10  $\mu\text{L}$  of a solution of “molecule 1” was made from a computer-controlled 300  $\mu\text{L}$  microsyringe at an interval of 400 s into the solution contained in the reaction cell, while stirring at 300 rpm at 25°C. The raw experimental data were reported as the amount of heat produced after each injection of boronic acid as a function of time. The amount of heat produced per injection was determined by integration of the area under individual peaks by the instrument software, after taking into account heat of dilution. The data were analysed using the one set of site fitting model (Origin 7.0 software package). Table S1 summarizes the experimental conditions used for the ITC measurements.

**Computational analysis.** Four possible trivalent PBA/maltose complexes (Figure 5), formed between the open glucose unit of the maltose derivative and PBA, have been studied: two bridged bicyclic compounds formed by 5- and 6-membered rings (complexes **2** and **4**) and two bridged bicyclic compounds formed by 5- and 7-membered rings (complexes **1** and **3**). For a better representation of the maltose derivative which is grafted to HA, C1 of the open glucose unit was replaced by a vinyl group. First, force field molecular dynamics (MD) simulations were carried out on the complexes for screening the different rotamers and rings conformations. The MD simulations were performed in the GROMACS software, ver. 2018,<sup>35</sup> with all-atom Gromos 54a7 force field.<sup>36</sup> All the MD simulations were performed in an NPT (constant number of atoms, pressure, and temperature) ensemble with velocity-rescale temperature coupling<sup>37</sup> and Berendsen pressure coupling algorithms<sup>38</sup> with temperature and pressure coupling constants of 0.2 ps and 2 ps, respectively. Each complex was placed in a box with dimensions with  $5 \times 5 \times 5$  nm<sup>3</sup> where single point charge (SPC) water molecules<sup>39</sup> are filled. The structure is then relaxed with energy minimization followed by MD simulation with slow heating from 0 K to 300 K in 2 ns. The system was then equilibrated for 8 ns at 300 K. The production run was performed for 10 ns at 300 K. Distributions of selected dihedral angles were summarized in Figure S33-36 in the supporting information. From the above MD simulations, the feasible conformers and rotamers of the different complexes were selected and submitted to DFT calculations using Gaussian 09 (rev. D.01)<sup>40</sup> with standard

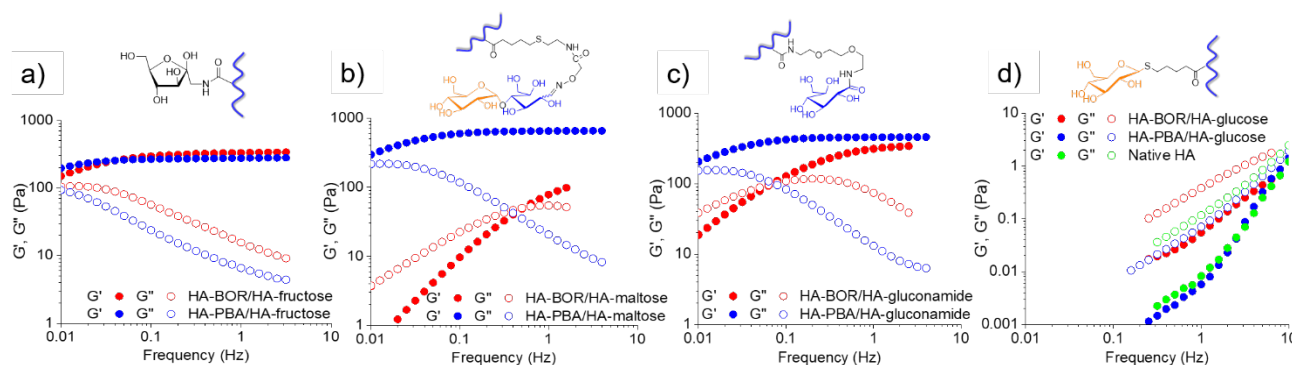


**Figure 2:** Frequency dependence of storage and loss moduli of networks based on (a) HA-PBA (BOR)/HA-fructose, (b) HA-PBA (BOR)/HA-maltose, (c) HA-PBA (BOR)/HA-gluconamide and (d) HA-PBA (BOR)/HA-glucose; closed symbols:  $G'$  curves; open symbols:  $G''$  curves.

termination options. Optimizations were performed with M062X<sup>41</sup> at 6-311+G(d,p) level and with SMD<sup>42</sup> in water. The functional was chosen for its proven performance in estimations of the relative energies of sugar conformers<sup>43,44</sup> and B-O bond length.<sup>45</sup> The SMD solvent simulation was chosen as it was shown to well reproduce the solvation effect.<sup>43</sup> For each DFT optimization, a frequency calculation was performed in order to verify that there is no negative frequency (i.e. confirm that it is a minimum) and to determine the absolute free energy of each rotamer at 298 K.

For the complexes of PBA and an open glucose used to simulate the gluconamide derivative (with the C1 replaced by a vinyl group, Figure S37), ten different trivalent possibilities have been studied: three bridged bicyclic compounds formed by two 5-membered rings and four bridged bicyclic compounds formed by 5- and 6-membered rings, one bridged bicyclic compound formed by two 6-membered rings and two bridged bicyclic compounds formed by 5- and 7-membered rings. In this case, only DFT calculation was performed for all possible rotamers of each complex, using the same condition described for the PBA/maltose derivative complexes.

For complexation between the grafted fructose and BOR with the open boroxole ring (Figure 4b), a 1-acetoamido fructose derivative was used to represent the amide bond between the monosaccharide and HA. Only MD simulation was carried out in the same condition as described for PBA/maltose derivative complexes.

## Results

### 1. Synthesis of the boronate ester-crosslinked networks and rheological characterization.

To properly compare the effect of the boronate ester crosslinker on the dynamic rheological properties of the HA networks, all HA derivatives were synthesized from the same initial HA sample, possessing a weight average molar mass  $M_w$  of 100 kg/mol, and with a similar degree of substitution (DS, average number of substituting group per repeating disaccharide unit) of 0.1-0.15 (see supporting information, Figure S1-S7, Table S2-S3). The different HA-based networks were produced by mixing thoroughly aqueous solutions of HA-PBA (or HA-BOR) and HA bearing saccharide moieties (HA-

maltose, HA-fructose, HA-glucose or HA-gluconamide) at physiological pH, at a total polymer concentration ( $C_p = 15$  g/L) higher than the overlap concentration of initial HA ( $C^* \approx 3$  g/L) and with a molar ratio of PBA (BOR)-to-grafted saccharide of 1. Dynamic rheological experiments revealed a gel-like behaviour ( $G' > G''$  in the frequency window explored) for the formulations based on HA-PBA (BOR)/HA-fructose (Figure 2a), HA-PBA/HA-maltose (Figure 2b) and HA-PBA/HA-gluconamide (Figure 2c). By contrast, HA-PBA and HA-BOR alone exhibited a viscous behaviour with  $G'$  and  $G''$  values similar to initial HA (Figure S8), confirming selective boronate ester crosslinking between PBA (BOR) and the sugar moieties grafted on HA.

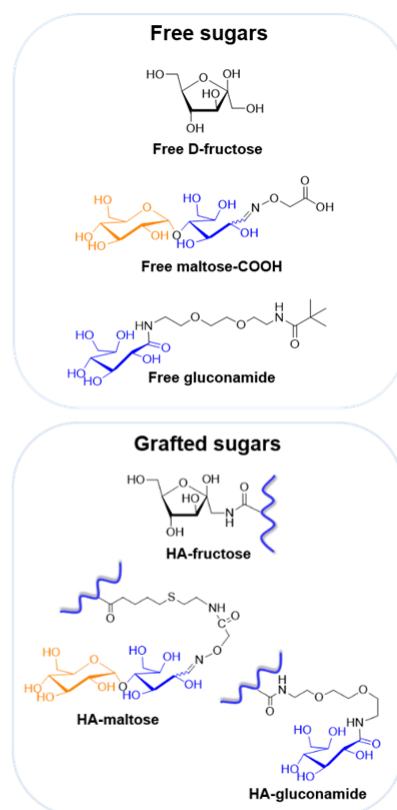
Quite surprisingly, in spite of the reported low binding constant of PBA with free maltose ( $K_a \sim 2.5$  L/mol)<sup>46</sup> compared to the  $K_a$  values of PBA with D-fructose ( $K_a \sim 128$ )<sup>46,47</sup> at physiological pH, the value of  $G'$  in the plateau region of the HA-PBA/HA-maltose network ( $G'_{1\text{Hz}} = 648$  Pa) is higher than the  $G'$  values of HA-PBA/HA-fructose assemblies ( $G'_{1\text{Hz}} = 276$ ). The same observation can be made for the HA-PBA/HA-gluconamide network, for which the value of  $G'$  in the plateau region is 558 Pa. These results suggest that, once grafted on HA, the mechanism of binding of PBA to the maltose is different from that of PBA to free maltose. This may be due to the ring-opened form of the glucose unit in the maltose derivative immobilized on the HA backbone. The rheological data obtained from the mixtures based on HA-glucose support this assumption (Figure 2d). These assemblies display a viscous behaviour ( $G'' > G'$  in the frequency window covered) which correlates with the low binding of PBA and BOR to free glucose ( $K_a \sim 5$  L/mol<sup>46</sup> and  $\sim 20$  L/mol<sup>24,48</sup>, respectively), which is mainly in the pyranose form (99.7 % in D<sub>2</sub>O and 27 °C)<sup>49</sup> in aqueous solution.

Another important observation is that the assemblies of HA-BOR with HA-maltose and HA-gluconamide have very different rheological properties compared to those obtained with HA-PBA. Indeed, viscoelastic behaviours (crossover of  $G'$  and  $G''$  seen within the tested frequencies) are observed for both HA-BOR mixtures (Figure 2b and 2c). These results are rather unexpected, especially in the case of the HA-BOR/HA-maltose since BOR is reported to have a higher binding affinity towards glycopyranosides than PBA.

From these rheological data, we can conclude that HA-BOR forms a gel-like network only with HA-fructose, whereas HA-PBA leads to gel-like networks with HA-fructose and HA

**Table 1:** Binding constants and/or exchange rate constants of complexes based on APBA/free fructose (free maltose-COOH), (free gluconamide), APBA/HA-fructose (HA-maltose) (HA-gluconamide), ABOR/free fructose (free maltose-COOH) (free gluconamide), ABOR/HA-fructose (HA-maltose) (HA-gluconamide).

Entry	Boronic acid	Saccharide	$K_a^a$ (L/mol)	$K_a^{b,c}$ ITC (L/mol)	$n^b$ (n saccharide : 1 boronic acid)	$k_{ex}$ ( $s^{-1}$ )
1	APBA	Free D-fructose	201 ± 5	112 ± 16	1.3 ± 0.3	0.66 ± 0.07 <sup>d</sup>
2	APBA	HA-fructose	503 ± 18			— <sup>e</sup>
3	ABOR	Free D-fructose	461 ± 73	484 ± 50	1.24 ± 0.1	0.18 ± 0.04 <sup>d</sup>
4	ABOR	HA-fructose	545 ± 28			— <sup>e</sup>
5	APBA	Free maltose-COOH	— <sup>f</sup>	2070 ± 146	0.46 ± 0.05	— <sup>g</sup>
6	APBA	HA-maltose	768 ± 71			0.27 <sup>d</sup>
7	ABOR	Free maltose-COOH	— <sup>h</sup>	305 ± 36	0.61 ± 0.3	184 <sup>i</sup>
8	ABOR	HA-maltose	— <sup>h</sup>			191 <sup>i</sup>
9	APBA	Free gluconamide	3220 ± 356	2340 ± 56	0.69 ± 0.01	— <sup>g</sup>
10	APBA	HA-gluconamide	1751 ± 221			0.20 <sup>d</sup>
11	ABOR	Free gluconamide	995 ± 125	933 ± 29	0.88 ± 0.03	— <sup>g</sup>
12	ABOR	HA-gluconamide	477 ± 132			— <sup>e</sup>



<sup>a</sup>  $K_a$  values measured from at least 1/10  $^1H$  NMR experiments, assuming formation of a 1:1 complex. <sup>b</sup>  $n$  value for free sugars measured from at least 1/10 ITC experiments. <sup>c</sup>  $K_a$  values for grafted sugars could not be measured by ITC because the thermodynamic parameters were affected by contributions from other effects related to the presence of the HA backbone. <sup>d</sup> measured using EXSY experiments. <sup>e</sup> not determined because of superposition of diagonal and cross-peaks arising from the bound and unbound APBA (ABOR) species. <sup>f</sup> not determined because the concentration of molecules used was too low to apply equations related to 1:2 equilibria. <sup>g</sup> not measured; <sup>h</sup> not measured because of rapid exchange dynamics relative to NMR timescale (extensive broadening of proton signals). <sup>i</sup> estimated from variable-temperature NMR experiments.

modified with glucose derivatives in the ring-opened form. On the basis of these observations, we investigated the relationships between the macroscopic mechanical properties of the HA assemblies and the small molecule crosslinkers by analysing the thermodynamics and the exchange kinetics of boronic acid-saccharide (fructose, maltose and gluconamide) complexation.

## 2. Thermodynamics and kinetics of boronic acid-saccharide complexation.

The binding constants were determined from  $^1H$  NMR titration and/or isothermal titration calorimetry (ITC) titration (see SI). Regarding the kinetics aspects, two-dimensional NMR exchange (2D EXSY) or variable-temperature NMR spectroscopy experiments were performed to quantify the molecular exchange dynamics (see SI). These experiments were performed with free and grafted sugars taking into account that the polymer backbone may influence complexation parameters.

**2.1. Complexation with free and grafted fructose.** NMR analysis (Figure S9-S12) of free 6-aminobenzoboroxole (hereinafter referred to as ABOR)/free fructose and ABOR/grafted fructose revealed similar association constants ( $K_a$ ) of 461 L/mol and 545 L/mol, respectively (Table 1, entries 3 and 4). In the case of free

3-aminophenylboronic acid (hereinafter referred to as APBA), its complexation with grafted fructose resulted in a 2.5-fold increase in the binding constant compared to the case with free fructose (Table 1, entries 1 and 2). Moreover, the  $K_a$  value for APBA/grafted fructose (503 L/mol) is relatively close to that measured for ABOR/grafted fructose. This is consistent with the fact that the  $G'$  values in the plateau region of HA-PBA/HA-fructose and HA-BOR/HA-fructose assemblies are similar (see Figure 2a). Indeed, as the plateau modulus scales with the number density of elastically active chains, its value strongly depends on the crosslink density, which is closely related to the binding constant of the PBA (BOR)/saccharide complex.

The binding constants for APBA/free fructose and ABOR/free fructose assessed by ITC were in the same order of magnitude as the values derived from  $^1H$  NMR (Table 1, entries 1 and 3). Additionally, 2D EXSY experiments revealed that the rates of chemical exchange for APBA/free fructose and ABOR/free fructose are in the same order of magnitude (0.66  $s^{-1}$  and 0.18  $s^{-1}$ , respectively, see Table 1, entries 1 and 3, Figure S13-S14). Such values correlate with the gel-like behaviour of these assemblies. In addition, the values are of the same order of magnitude as those previously reported in a study on bulk materials based on a diol-containing polymer cross-linked by

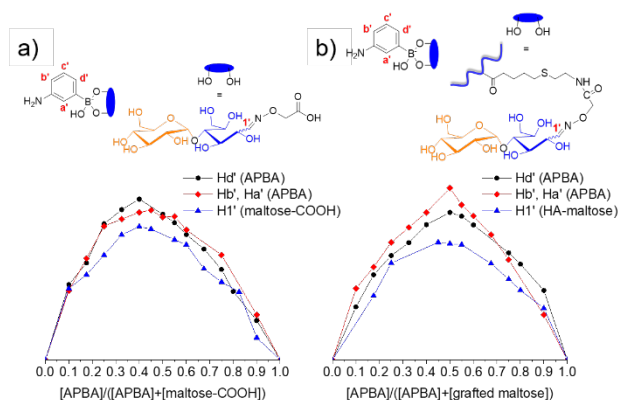


**Figure 3:**  $^1\text{H}$  NMR Job plots for (a) APBA/maltose-COOH and, for (b) APBA/grafted maltose (HA-maltose), showing a maximum at a molar ratio of 0.4 and 0.5, respectively.

telechelic diboronate ester crosslinkers.<sup>25</sup> In these systems, highly elastic properties were obtained using a diboronate ester crosslinker with a transesterification rate of  $0.016\text{ s}^{-1}$ , while a viscoelastic behaviour was observed with a crosslinker possessing a transesterification rate of  $3000\text{ s}^{-1}$ . It should be noted here that the values were determined from the free molecules. We cannot exclude slight variations when boronic acid and fructose moieties are grafted on the HA backbone.

**2.2. Complexation with free and grafted maltose.** With regard to the binding of APBA and ABOR to free maltose-COOH and grafted maltose (HA-maltose), NMR and ITC analysis (Figure S15-S20) showed strikingly high affinity of APBA for free maltose-COOH and grafted maltose (Table 1, entries 5 and 6).

In the case of the APBA/maltose-COOH system, analysis of the ITC data with a one-site binding model gave a  $K_a$  value of  $2070\text{ L/mol}$  and a stoichiometry  $n$  ( $n$  saccharide:1 boronic acid) of 0.46. By using the method of continuous variation (also referred as Job's method),<sup>51</sup> we were able to confirm a deviation from the 1:1 stoichiometry for the APBA/maltose-COOH pair in contrast to grafted maltose. In fact, as shown in Figure 3, a maximum at a molar fraction of  $\sim 0.4$  is observed, indicating a composite binding stoichiometry.<sup>52</sup> In the case of the APBA/grafted maltose the Job plot indicated a maximum at 0.5. Assuming formation of a 1:1 complex for the APBA/grafted maltose pair, a binding constant of  $768\text{ L/mol}$  was found from  $^1\text{H}$  NMR analysis (Table 1, entry 6). The relatively high  $K_a$  values compared to the binding affinity of PBA towards free maltose<sup>46</sup> are probably connected with the difference in the structure between this sugar and the free maltose-COOH derivatives. The latter consists of a terminal  $\alpha$ -D-glucopyranoside unit linked to a ring-opened glucose unit while it is well-known that, in free maltose, this first glucose unit is mostly in the pyranose form. In the case of ABOR/maltose-COOH complexation, ITC analysis also revealed significant deviation from 1:1 stoichiometry (Table 1, entry 7). This suggests the possibility that two ABOR molecules are bound to the maltose derivative.  $^1\text{H}$  NMR experiments further showed that the rate of chemical exchange is slower for APBA/HA-maltose than for ABOR/HA-maltose. As seen from Table 1, the rate of chemical exchange for APBA/grafted maltose was found to be much lower than that

for ABOR/grafted maltose ( $0.27\text{ s}^{-1}$  and  $191\text{ s}^{-1}$ , respectively, see entries 6 and 1 in Table 1, Figure S21-S23). This difference in molecular exchange kinetics between the complexes may provide an explanation for the gel-like behaviour of the HA-PBA/HA-maltose assembly compared to the viscoelastic behaviour observed for HA-BOR/HA-maltose.

### 2.3. Complexation with free and grafted gluconamide.

Interestingly, the results obtained from the analysis of the binding of APBA and ABOR to free and grafted gluconamide (HA-gluconamide) supported our assumption that the ring-opened form of the glucose unit in the maltose derivative is partly responsible for its strong interaction with APBA (Figure S24-S27). The interaction of APBA with free gluconamide produced a complex with a  $K_a$  value nearly two orders of magnitude higher than that with free fructose (Table 1, entries 1 and 9, Figure S24). The Job plot for APBA and free gluconamide indicated the formation of a complex with a stoichiometry of 1:1 with a maximum at 0.5 (Figure S28). Although a decrease of the  $K_a$  value is observed once the gluconamide derivative is grafted on HA (Table 1, entry 10), it remains high compared to association constants reported for the binding of PBA to various natural mono- and disaccharides which do not exceed  $400\text{ L/mol}$ .<sup>46</sup> The interaction of ABOR with free gluconamide also resulted in a binding constant significantly higher than that with free fructose (Table 1, entries 2 and 10, Figure S29). However, superposition of cross-peaks in the 2D EXSY spectrum precluded quantification of  $k_{ex}$  for ABOR/gluconamide.

Collectively, these results demonstrate the high binding capacity of PBA towards glucose units in the ring-opened form (i.e. the maltose and gluconamide derivatives), resulting in the formation of complexes with slow exchange dynamics. However, in view of the different binding constant and stoichiometry values found for the APBA/maltose-COOH and APBA/free gluconamide complexes, it can be reasonably assumed that the binding mechanism of PBA to the maltose is different compared to gluconamide derivatives. Moreover, another striking result is the high binding capacity of APBA towards fructose when grafted on HA, which results in the formation of a hydrogel network with dynamic rheological properties similar to the network based on BOR/fructose crosslinks.

**Table 2:** Summary of the rheological, thermodynamic and kinetic properties of the boronate cross-linked hydrogels.

	APBA (HA-PBA)	ABOR (HA-BOR)
Fructofuranose (HA-fructose)	"Strong" gel $K_a > 100\text{ L/mol}$ , $k_{ex} < 1\text{ s}^{-1}$	"Strong" gel $K_a > 100\text{ L/mol}$ , $k_{ex} < 1\text{ s}^{-1}$
Ring-open glucose (HA-gluconamide, HA-maltose)	"Strong" gel $K_a > 100\text{ L/mol}$ , $k_{ex} < 1\text{ s}^{-1}$	"Viscoelastic" gel $K_a > 100\text{ L/mol}$ , $k_{ex} > 1\text{ s}^{-1}$
Glucopyranose (HA-glucose)	No gel $K_a < 100\text{ L/mol}$ <sup>a</sup>	No gel $K_a < 100\text{ L/mol}$ <sup>a</sup>

<sup>a</sup> Information based on literature values:  $K_{a\text{PBA}} \sim 5\text{ L/mol}$ ,<sup>46</sup>  $K_{a\text{BOR}} \sim 20\text{ L/mol}$ .<sup>24,48</sup>

Table 2 summarizes the rheological behaviours of the different networks and the kinetic and thermodynamic parameters corresponding to the small molecular crosslinkers.

### 3. Determination of the structures of the boronic acid complexes with fructose and glucose-like molecules grafted on HA.

To gain more insight into the binding mode of PBA to the fructose, maltose and gluconamide derivatives which is connected with the unexpected macroscopic mechanical properties, we studied the structures of the boronic acid complexes by NMR and molecular modelling.

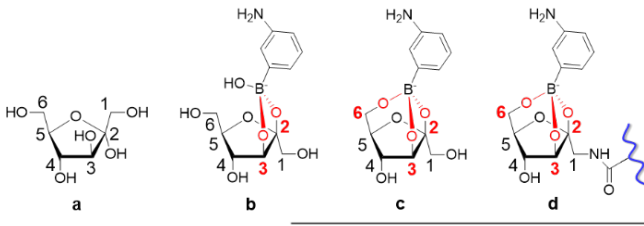
**3.1. Complexes with free and grafted fructose.** The binding mode of APBA towards fructose grafted on HA could be readily determined from  $^{13}\text{C}$  NMR spectroscopy based on the  $^{13}\text{C}$  chemical shift values reported by Norrild *et al.* for different PBA/fructose complexes formed in neutral and alkaline aqueous solutions.<sup>53</sup> These authors assigned the structures of the complexes in solution on the basis of  $^1J_{\text{CC}}$  coupling constants which provided information of the binding sites for the formed cyclic boronate esters. In our study, comparison of the  $^{13}\text{C}$  chemical shifts of the 1:1 complexes formed between D-fructose and APBA in  $\text{D}_2\text{O}$  (pD 7.4 and pD 11-12) with those of APBA in the presence of HA-fructose ( $[\text{PBA}]/[\text{fructose}] = 1$ , pD 7.4) showed that APBA mainly binds the fructose moiety grafted on HA in a trivalent fashion, similar to the APBA/D-fructose complex in alkaline conditions (Table 3 and Figure S29). This binding mode was evidenced by the upshift of the C6 signal of bound fructose (mainly in the furanose form) from 62.4 to 65 ppm, observed for both the APBA/D-fructose complex (pD = 11-12, Table 3) and APBA/HA-fructose (pD = 7.4, Table 3). This upshift is due to bond formation between the C6-OH group and boron in addition to B-O bond formation between the C2-OH and C3-OH of fructose. This is a rather surprising result which, however, fully supports the assumption that the HA backbone may contribute to the increased binding affinity of PBA for grafted fructose (section 2.1).

The binding mode of ABOR towards free (grafted) fructose was also investigated by  $^1\text{H}$  and  $^{13}\text{C}$  NMR at physiological pH. Surprisingly, the complexation between ABOR and fructose was found to involve the opening of the endocyclic B-O bond of ABOR. This was demonstrated by comparing the  $^1\text{H}$  NMR spectra of ABOR alone in the open form (i.e. at pD 11-12)<sup>30</sup> and in the closed form (at pD 7.4) as well as of ABOR in the presence of free D-fructose (Figure S30a) and grafted fructose (HA-fructose, Figure S30b) at pD 7.4. The upshift observed for the  $\text{CH}_2\text{O}$  group of ABOR in the presence of both free/grafted fructose similar to that of ABOR alone at alkaline pH indeed provided evidence of the opening of the oxaborole ring. Further 2D INADEQUATE NMR experiments using  $^{13}\text{C}$  labelled D-fructose revealed that ABOR forms a vicinal cyclic boronate ester with the *syn*-periplanar anomeric hydroxyl pair (C2–C3) of D-fructose (Figure 4a, Figure S31). The formation of this bidentate complex with fructose (mainly in the furanose form) was evidenced by a significant decrease in the  $^1J_{\text{C2-C3}}$  value of the bound  $\beta$ -D-fructofuranose form. Indeed, exceptionally low values for  $^1J_{\text{CC}}$  are measured for vicinal diols when the O-C-C-O

fragment becomes incorporated in a five-membered ring, as is the case for vicinal cyclic boronate esters.<sup>54</sup> It is also worth noting that upon complexation with ABOR, the C2 and C3 carbon signals of  $\beta$ -D-fructofuranose experience the largest chemical shift changes, similar to those observed for complexation of APBA with D-fructose/grafted fructose at pD 7.4, whereas no chemical shift change is observed for the C6 carbon of  $\beta$ -D-fructofuranose (Figure 4a, NMR data summarized in the Table). Collectively, these data demonstrate that complexation of ABOR with fructose leads to the formation of a monocyclic adduct instead of a spiro adduct due to the opening of the oxaborole ring. Based on these results, we performed molecular dynamics (MD) simulations to determine whether any preferred conformation can explain the stability of the bidentate complex with the opened oxaborole ring. For a better representation of the sugar grafted to HA, the bidentate complex was simulated using a  $\beta$ -D-fructofuranose with an acetamide group replacing OH-1. As it can be seen in Figure 4b, a strong hydrogen bond (average  $\text{D}_\text{O}\cdots\text{A}$  distance = 2.5 Å,  $\text{D}_\text{H}\cdots\text{A}$  distance = 1.7 Å and  $\text{D}_\text{O}-\text{H}\cdots\text{A}$  angle = 11°) is formed between the O3 of the bound fructose part and the  $\text{CH}_2\text{-OH}$  group in the open oxaborole ring. The occupancy of this hydrogen bond over the simulation time is nearly 1, indicating the robustness of this conformation. Furthermore, a second weaker hydrogen bond between the B-OH and the OH-6 group of fructose helps stabilizing this conformation, which is unfavourable for reverting the reaction toward the closure of the oxaborole ring.

**3.2. Complexes with free and grafted glucose-like molecules.** In order to elucidate the binding mode of APBA with grafted maltose, the chemical shifts and  $^1J_{\text{CC}}$  coupling constants of grafted maltose in the absence and in the presence of APBA were measured on an ultra-high field NMR spectrometer (950 MHz). We used a  $^{13}\text{C}$ -edited HSQC experiment, which allows the selective detection of  $^1\text{H}$  signals attached to labelled  $^{13}\text{C}$ . To this end, a  $^{13}\text{C}$  labelled maltose derivative was grafted on HA. Comparison of the  $^{13}\text{C}$ -edited HSQC spectrum of the 1:1

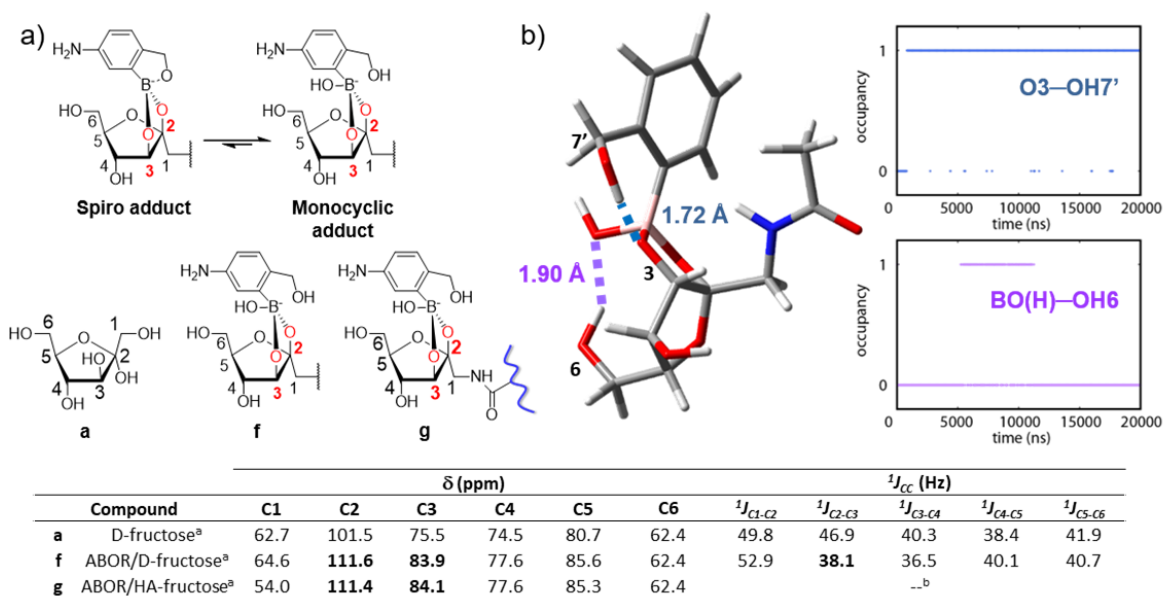
**Table 3:**  $^{13}\text{C}$  chemical shifts ( $\delta$  in ppm) for D-fructose and grafted fructose (HA-fructose) a one and/or bound to APBA in  $\text{D}_2\text{O}$ . Entries in bold correspond to values that display an upshift due to complexation.



Compound	pD	$\delta$ (ppm)					
		C1	C2	C3	C4	C5	C6
a D-fructose <sup>a</sup>	7.4	62.7	101.5	75.5	74.5	80.7	62.4
b APBA/D-fructose <sup>a</sup>	7.4	63.6	<b>110.3</b>	<b>82.4</b>	79.1	85.0	62.4
c APBA/D-fructose <sup>a</sup>	11-12	63.2	<b>110.5</b>	<b>81.9</b>	79.3	84.8	<b>65.1</b>
d APBA/HA-fructose <sup>a</sup>	7.4	53.6	<b>109.8</b>	<b>81.5</b>	79.4	84.8	<b>65.0</b>

<sup>a</sup>The  $\delta$  values are given for  $\beta$ -D-fructofuranose (with CH<sub>2</sub> as the major tautomeric form observed for grafted fructose moieties (HA-fructose, see SI)).





<sup>a</sup>The  $\delta$  values are given for  $\beta$ -D-fructopyranose which is the major tautomeric form observed for grafted fructose moieties (HA-fructose, see SI). <sup>b</sup>Not determined because  $^1J_{CC}$  values were only measured using  $^{13}C$  labeled D-fructose.

**Figure 4:** (a) Structures and assignment of experimental  $^{13}C$ -NMR data ( $D_2O$ , pD 7.4) of D-fructose and grafted fructose (HA-fructose) alone and/or bound to ABOR:  $^{13}C$  chemical shifts ( $\delta$  in ppm, entries in bold correspond to values that display an upshift due to complexation) and  $^1J_{CC}$  coupling constants (in Hz). (b) Conformational screening of the complex formed by BOR (with the open oxaborole ring) and fructose by classical MD simulations (with all-atom GROMOS force field performed using GROMACS software): preferred conformation of the BOR/fructose complex stabilized by two hydrogen bonds (blue and violet dashed lines); and occupancy in time of the hydrogen bonds O3-OH7' (blue) and BO(H)-OH6 (violet).

complex formed between grafted maltose and APBA and the spectrum of grafted maltose alone in  $D_2O$  (pD 7.4) revealed no change in the chemical shift for all  $^{13}C$  of the terminal glucopyranose unit, suggesting no complexation with this sugar unit (Table S4-S5, Figure S32). In contrast, an upshift of the C6 signal of the open sugar unit was observed. Unfortunately, as this highly flexible sugar likely leads to the formation of several complexes with APBA, their presence at very small concentration hampers their detection by NMR. Thus, the other  $^{13}C$  signals detected were found to have the same chemical shifts as those of the open sugar unit in the absence of APBA. Therefore, it was not possible to draw conclusions about the hydroxyl groups of this sugar involved in the formation of a complex with APBA except the OH-6. Having a look at the values of  $^1J_{CC}$  of the open glucose unit of grafted maltose in the presence of APBA, it can be noted that they are similar to those measured in the absence of APBA (Table S5). This can be explained by the flexible structure of open glucose unit of grafted maltose, which does not cause significant changes in the torsional angles upon complexation.

To support the assumption that only the glucose unit which is in the open form is involved in the binding mode of grafted maltose with APBA, density functional theory (DFT) calculations were performed on the different possible complexes formed between APBA and grafted maltose, in order to determine which binding mode is the most stable. To simplify the molecules for the calculations, complexes were simulated using the PBA molecule and a model of the maltose derivative possessing a vinyl group replacing the C1 of its open glucose unit. The solvent model density (SMD)<sup>42</sup> method was used to

simulate the aqueous environment of the complexes. The fact that the stoichiometry of  $\sim 2:1$  measured for APBA/free maltose-COOH changes to 1:1 when maltose is grafted on HA (Figure 3 and Table 1, entry 5) suggests that the binding mode of PBA towards free/grafted maltose changes. It can be assumed that a trivalent complex is obtained with the maltose derivative grafted on HA, similar to that observed for free/grafted fructose (Table 3). This is supported by the fact that a slow network dynamics is observed with HA-maltose similar to HA-fructose. Based on this assumption, only trivalent complexes formed between PBA and the open glucose unit of the grafted maltose derivative were taken into consideration for the calculations.

When simulating a possible complex of PBA bound to the open and closed glucose units of the disaccharide model (including C5-OH, C6-OH and C6'-OH as binding sites, see structure of the maltose derivative in Figure 5), a free energy above 15 kcal/mol was obtained with respect to the energy of the most stable complex (data not shown). This indicates that this binding mode is not the most stable for PBA/grafted maltose, which fully supports the NMR observations. This result may be explained by the fact that the binding of PBA to the glucopyranose ring would require the formation of cycles with a large size, including at least an 8-membered ring (which is known to be less favourable than 5- or 6-membered cycles).

Based on this, we focused on studying the 4 possible bridged bicyclic compounds formed by a trivalent complexation between the open glucose unit of maltose and PBA (complexes 1-4, Figure 5). Prior to DFT calculations, MD studies were performed on each complex in order to reduce the number of conformers which includes rotamers (see SI, Figure S33-S36).

DFT calculations suggested that the four possible complexes may exist at room temperature, as there are only 2 kcal/mol of difference of free energy between the most stable and the less stable binding modes (Figure 5).

Surprisingly, complex **1** (a 5- and 7-membered bridged bicyclic compound) was found to be as stable as complex **2** (a 5- and 6-membered bridged bicyclic compound). This unexpected result could be explained by an intramolecular hydrogen bond formed between the only free hydroxyl group of the open chain glucose and an oxygen atom in the phenylboronate ester, thus stabilizing the bicyclic compound. These results confirm that various binding modes may exist for PBA/grafted maltose, which correlates with the fact that their NMR spectrum could not be easily interpreted.

When performing the same study using a gluconamide model (an open glucose with a vinyl group replacing the C1), we observed that among ten possible tricovalent complexes, only five showed a significant population at room temperature, and four of them were the corresponding analogues of the PBA/maltose complexes (Figure S37). It should be noted that the values of  $\Delta G$  between these five complexes are very low.

With regard to the binding mode of BOR to the maltose derivative in HA-BOR/HA-maltose network, because of the steric hindrance caused by the HA chains, it can be reasonably assumed that only complexes with a stoichiometry of 1:1 are formed. Besides possible binding to the terminal glucopyranose unit as discussed above, BOR may also form complexes with the open glucose unit. In the latter case, considering the most stable structures of the complexes determined for PBA/grafted maltose, we would expect the formation of five structures as dicovalent complexes (Figure S38). It should be noted that in this case, no upfield shift of the CH<sub>2</sub>O group was observed for BOR in the presence of HA-maltose in comparison to BOR alone (Figure S39). This indicates that BOR is mainly in the closed form.

A different situation was observed from the <sup>1</sup>H NMR analysis of complexes of BOR with free/grafted gluconamide. Although

extensive broadening of proton signals was observed in the NMR spectra of the complexes, it was possible to distinguish both the closed and open forms of ABOR (Figure S40). Despite the fact that the open form of ABOR represents a very small fraction and that the flexible open chain glucose derivative can adopt various conformations, the existence of a small proportion of monocyclic adduct due to the opening of the oxaborole ring, besides spiro adducts, cannot be excluded. Therefore, looking at the complexes of PBA/gluconamide, we would expect that the complexation between BOR and gluconamide would include at least nine possible binding modes in a dicovalent fashion involving the cyclic form of BOR (spiro adducts). Nevertheless, as discussed above, we cannot exclude that other binding modes would exist including the open form of BOR.

## Discussion

In recent years, the desire to rationally control the properties of injectable hydrogels has promoted the emergence of new synthetic and natural polymer networks crosslinked via ester bond formation between boronic acid derivatives and glucose-like diols.<sup>9, 15, 16, 19, 21, 22, 55</sup> In this regard, Yesilyurt et al. obtained a poly(acrylamide)-based injectable system exhibiting a gel-like behaviour via complexation between APBA and glucose in the ring-opened form.<sup>19</sup> These results are consistent with our findings, which highlights the anomalously high binding profile for glucose (in the ring-opened form)-APBA complexation.

Our work additionally points out the fact that the  $pK_a$  of phenylboronic acid derivatives is not a reliable factor that determines rheological properties of boronate ester-crosslinked networks. This is clearly demonstrated by the comparative analysis of the networks based on HA-PBA and HA-BOR. When HA-maltose and HA-gluconamide are used as partners of HA-PBA and HA-BOR, a gel-like behaviour was only observed for the assemblies based on HA-PBA, despite the lower  $pK_a$  of ABOR compared to APBA. The viscoelastic

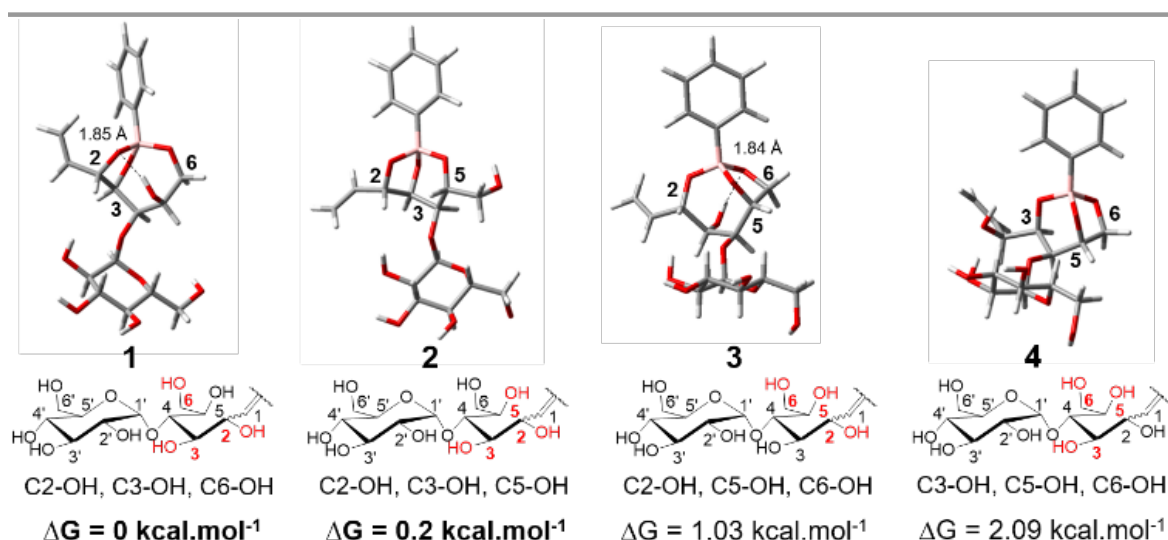


**Figure 5:** Optimized structures (M062X/6-311+G(d,p) SMD) of most stable complexes between PBA and maltose derivative. Note: The indicated values of energy are relative ones, with the minimum set at 0 kcal/mol for the respective lowest energy structures of the binding mode 1.

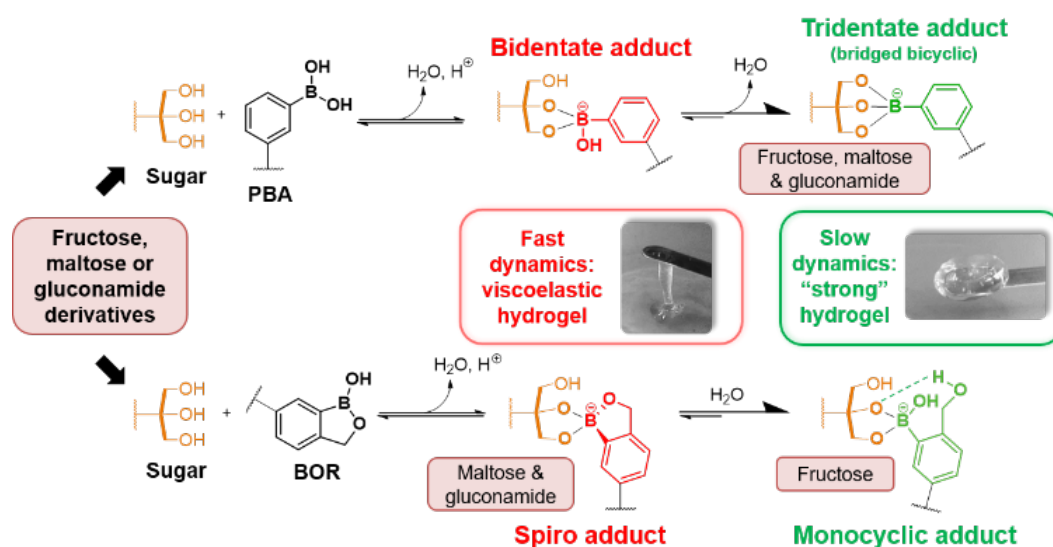


Figure 6: Proposed mechanism explaining the dynamics of the HA networks in relation to the small molecular cross-linkers at physiological pH

behaviour observed for the assemblies based on HA-BOR/HA-maltose (gluconamide) is in full agreement with rheological data reported previously for synthetic polymer networks crosslinked via glucose (in the ring-opened form)-BOR complexation.<sup>21, 22</sup> All these results led us to conduct mechanistic studies of the molecular contributions to the rheological dynamic properties of the hydrogel networks.

From the rheological data shown in Figure 2 and the  $k_{ex}$  values given in Table 1, it can be observed that the inverse of  $k_{ex}$  is related to the characteristic relaxation time of the network  $\tau_N$  (defined by  $\tau_N = (\omega_c)^{-1}$  and  $\omega_c$ , the crossover frequency where  $G' = G''$ )<sup>27, 56</sup>. Thus, boronate ester bonds with a low  $k_{ex}$  ( $\sim 0.2$ - $0.7$  s<sup>-1</sup>) produce gel-like networks whereas boronate ester bonds with a higher  $k_{ex}$  ( $\sim 180$ - $190$  s<sup>-1</sup>) generate viscoelastic networks ( $\omega_c$  seen in the frequency range of 0.01 to 10 Hz). Moreover, though similar binding constants were found for ABOR/HA-fructose and ABOR/HA-gluconamide, dynamic rheology revealed a gel-like behaviour for HA-BOR/HA-fructose and viscoelastic properties for HA-BOR/HA-gluconamide. Similar observations were reported by Lin et al. in a study on hydrogels formed from BOR-containing poly(acrylamides) and three glycopolymers possessing an identical main chain but different pendent sugars.<sup>9</sup> Indeed, these authors found that the binding constants between BOR and the sugars did not show any significant impact on the dynamics of the polymer assemblies. These data make us really believe that the molecular exchange kinetics of the boronic ester crosslinks is the primary determinant of the relaxation dynamics of the HA assemblies. This is in line with theoretical studies showing that the dynamics of reversible networks is governed primarily by the network strand size and by the effective lifetime of reversible junctions.<sup>57-59</sup>

To better understand the different dynamic rheological properties observed, an analysis of the binding mode of PBA and BOR toward the different saccharide moieties grafted on HA at physiological pH was performed by NMR and computational analysis.

From these analyses performed on the complexes of APBA with free and grafted fructose, it can reasonably be inferred that the higher binding affinity of APBA for fructose grafted on HA than for free fructose is due to the formation of a tricovalent ester. A tridentate complex with a 1:1 stoichiometry also seems to be formed between APBA and maltose grafted on HA, in accordance to the high association constant recorded for this complex. Finally, the high binding affinities obtained for complexation of APBA with the free and grafted gluconamide derivatives also strongly suggest formation of tricovalent adducts. In this respect, literature data show that the stability of borate-carbohydrate complexes increases with the number of coordination sites (tridentate > bidentate > monodentate).<sup>60</sup> In these systems, we believe that the formation of tricovalent adducts is a major cause of the slow network exchange kinetics (Figure 6). This is supported by a recent study showing fast relaxation dynamics for PEG networks crosslinked via boronate ester bonds between catechol and PBA moieties grafted on the PEG derivatives.<sup>14</sup> Catechols have special features in that their structure precludes formation of tridentate complexes on the one hand, and that they bind with boronic acids with much higher affinities than most carbohydrates, on the other.<sup>18</sup> Based on this, we examined formation of networks by combining HA-PBA with HA modified with catecholamine (dopamine)<sup>61</sup> and interestingly, fast network relaxation was also observed in this case (Figure S41).

Regarding the HA-BOR/HA-fructose network, our results indicate that its slow dynamics is related to the original and previously unobserved binding mode between BOR and fructose, leading to the formation of a monocyclic adduct instead of a spiro adduct due to the opening of the oxaborole ring (Figure 6). This adduct is stabilized by strong hydrogen bonding. This phenomenon is more specifically observed with fructose, which may be due to the locally optimized geometry of the hydroxyl groups of its  $\beta$ -D-fructofuranose tautomeric form. This favours the formation of a bidentate complex with the *cis*-1,2 diol.

In the case of the HA-BOR/HA-maltose and HA-BOR/HA-gluconamide mixtures, a more rapid molecular exchange dynamics is observed which can be attributed to formation of classical spiro adducts. The strained spiro structure may promote B-O bond cleavage and thereby, complex dissociation. Nevertheless, as the neutral, trigonal planar boron atom is also constrained in the uncomplexed five-membered oxaborole ring, spiro adducts are rapidly re-formed. It is indeed believed that the ring strain in the oxaborole heterocyclic ring is at the origin of the decrease in  $pK_a$  in comparison to PBA as the ring strain is relieved upon ionization.<sup>62, 63</sup> This phenomenon may result in rapid molecular exchange kinetics (Figure 6). This is in contrast to the complexes with PBA which consist of more stable bridged bicyclic compounds. Finally, although it is difficult to have a clear picture of the binding mode of BOR to gluconamide, we hypothesize that the formation of a monocyclic adduct in a small proportion with respect to “classical” spiro adducts may account for the slower dynamics observed for the HA-BOR/HA-gluconamide assemblies in comparison to the HA-BOR/HA-maltose ones.

One question remains with regard to the formation of a trivalent APBA/fructose complex rather than a divalent one when fructose is grafted on HA. While it has been traditionally thought that boronate ester formation proceeded through the boronate anion exclusively,<sup>18</sup> more recent studies showed that the kinetically preferred pathway to the boronate ester species is via trigonal boronic acid.<sup>64, 65</sup> In this latter case, the neutral diester formed by reaction of trigonal boronic acid and the diol-containing molecule reacts with a water molecule in a second step to produce the anionic tetrahedral diester adduct (Figure S42).

Building on these findings, it can be inferred that the environment created by HA makes the OH-6 group of fructose more efficient to react with the neutral diester intermediate than water. The high water-binding capacity of HA may provide some explanation for this. Indeed, it can be assumed that the water molecules organized near the polysaccharide chains—tightly bound and weakly bound water via formation of hydrogen bonds with HA,<sup>66-69</sup> decreases ability of water to react with neutral boronate ester species. As a result, the formation of trivalent complexes with fructose as well as with the maltose and gluconamide derivatives grafted on HA is favoured. With this hypothesis, efficient boronate ester crosslinking via trivalent complex formation should be also observed with other derivatives of highly hydrated polymers. In this regard, we previously reported efficient boronate ester crosslinking upon mixing PBA- and maltose-linked carboxymethylcellulose (CMC) derivatives.<sup>15</sup> Similarly to HA-PBA/HA-maltose, the CMC-PBA/CMC-maltose mixture displayed a gel-like behaviour in the frequency window explored.

## Conclusion

In this study, we demonstrated the outstanding capability of 3-aminophenylboronic acid to bind fructose and open chain glucose derivatives grafted on hyaluronic acid, resulting in the

formation of hydrogel networks with slow relaxation times and relatively high dynamic moduli. The correlation between the structure of the APBA/carbohydrate complexes and their thermodynamics and molecular exchange dynamics reveals the importance of the trivalent binding mode for efficient boronate ester crosslinking in HA hydrogels. Notably, the previously unobserved trivalent structure of complexes with APBA at physiological pH plays a key role in increasing the lifetime of the small molecular crosslinkers. Remarkably, we also found that complexation of 6-aminobenzoboroxole with fructose results in a monocyclic adduct instead of a spiro adduct as observed with other carbohydrates, leading to the formation of hydrogel networks that feature slow relaxation dynamics compared to the other assemblies formed by complexation of BOR and glucose-derivatives grafted on HA. Furthermore, we also demonstrated that the polymer backbone on which the boronic acid and sugar moieties are grafted can also affect the structure of the boronate complexes. This is highlighted here in the case of the APBA/fructose complexation.

Our study shows the ability to tune the viscoelastic properties of boronate-crosslinked HA hydrogels according to the boronic acid derivative/sugar pair. This paves the way for developing versatile platforms that can, for example, mimic the dynamic aspects of cellular microenvironments.

## Conflicts of interest

There are no conflicts to declare

## Acknowledgements

This work was supported by Galderma-Nestlé Skin Health. The authors thank Dr. C. Bouix-Peter at Galderma R&D for valuable discussions; the NMR platform of ICMG (FR2607) for its support; the CECIC Cluster (ICMG) used to perform MD simulations and DFT calculations; the IBS high-field NMR spectroscopy platform and Dr. Bernhard Brutscher at this NMR Platform for the <sup>13</sup>C-edited HSQC experiments (950 MHz).

## Notes and references

1. Taylor, D. L.; in het Panhuis, M., Self-Healing Hydrogels. *Advanced Materials* **2016**, *28* (41), 9060-9093.
2. Wang, H.; Heilshorn, S. C., Adaptable Hydrogel Networks with Reversible Linkages for Tissue Engineering. *Advanced Materials* **2015**, *27* (25), 3717-3736.
3. Loebel, C.; Rodell, C. B.; Chen, M. H.; Burdick, J. A., Shear-thinning and self-healing hydrogels as injectable therapeutics and for 3D-printing. *Nat. Protoc.* **2017**, *12* (8), 1521-1541.
4. Jin, Y.; Yu, C.; Denman, R. J.; Zhang, W., Recent advances in dynamic covalent chemistry. *Chem. Soc. Rev.* **2013**, *42* (16), 6634-6654.
5. Deng, C. C.; Brooks, W. L. A.; Abboud, K. A.; Sumerlin, B. S., Boronic Acid-Based Hydrogels Undergo Self-Healing at Neutral and Acidic pH. *ACS Macro Lett.* **2015**, *4* (2), 220-224.
6. He, L.; Fullenkamp, D. E.; Rivera, J. G.; Messersmith, P. B., pH responsive self-healing hydrogels formed by boronate-catechol

- complexation. *Chemical Communications (Cambridge, United Kingdom)* **2011**, 47 (26), 7497-7499.
7. Kitano, S.; Kataoka, K.; Koyama, Y.; Okano, T.; Sakurai, Y., Glucose-responsive complex formation between poly(vinyl alcohol) and poly(N-vinyl-2-pyrrolidone) with pendent phenylboronic acid moieties. *Makromol. Chem., Rapid Commun.* **1991**, 12 (4), 227-33.
  8. Kotsuchibashi, Y.; Agustin, R. V. C.; Lu, J.-Y.; Hall, D. G.; Narain, R., Temperature, pH, and Glucose Responsive Gels via Simple Mixing of Boroxole- and Glyco-Based Polymers. *ACS Macro Lett.* **2013**, 2 (3), 260-264.
  9. Lin, M.; Sun, P.; Chen, G.; Jiang, M., The glyco-stereoisomerism effect on hydrogelation of polymers interacting via dynamic covalent bonds. *Chemical communications* **2014**, 50 (68), 9779-82.
  10. Meng, H.; Xiao, P.; Gu, J.; Wen, X.; Xu, J.; Zhao, C.; Zhang, J.; Chen, T., Self-healable macro-/microscopic shape memory hydrogels based on supramolecular interactions. *Chemical Communications* **2014**, 50 (82), 12277-12280.
  11. Pettignano, A.; Haring, M.; Diaz Diaz, D.; Grijalvo, S.; Eritja, R.; Tanchoux, N.; Quignard, F., Boronic acid-modified alginate enables direct formation of injectable, self-healing and multistimuli-responsive hydrogels. *Chemical communications* **2017**, 53 (23), 3350-3353.
  12. Roberts, M. C.; Hanson, M. C.; Massey, A. P.; Karren, E. A.; Kiser, P. F., Dynamically restructuring hydrogel networks formed with reversible covalent crosslinks. *Advanced Materials* **2007**, 19 (18), 2503-2507.
  13. Shan, M.; Gong, C.; Li, B.; Wu, G., A pH, glucose, and dopamine triple-responsive, self-healable adhesive hydrogel formed by phenylborate-catechol complexation. *Polym. Chem.* **2017**, 8 (19), 2997-3005.
  14. Tang, S.; Ma, H.; Tu, H.-C.; Wang, H.-R.; Lin, P.-C.; Anseth, K. S., Adaptable Fast Relaxing Boronate-Based Hydrogels for Probing Cell-Matrix Interactions. *Advanced Science* **2018**, 5 (9), n/a.
  15. Tarus, D.; Hachet, E.; Messenger, L.; Catargi, B.; Ravaine, V.; Auzely-Velty, R., Readily Prepared Dynamic Hydrogels by Combining Phenyl Boronic Acid- and Maltose-Modified Anionic Polysaccharides at Neutral pH. *Macromol. Rapid Commun.* **2014**, 35 (24), 2089-2095.
  16. Yesilyurt, V.; Webber, M. J.; Appel, E. A.; Godwin, C.; Langer, R.; Anderson, D. G., Injectable Self-Healing Glucose-Responsive Hydrogels with pH-Regulated Mechanical Properties. *Advanced Materials* **2016**, 28 (1), 86-91.
  17. Marco-Dufort, B.; Tibbitt, M. W., Design of moldable hydrogels for biomedical applications using dynamic covalent boronic esters. *Mater. Today Chem.* **2019**, 12, 16-33.
  18. Yan, J.; Springsteen, G.; Deeter, S.; Wang, B., The relationship among pKa, pH, and binding constants in the interactions between boronic acids and diols-it is not as simple as it appears. *Tetrahedron* **2004**, 60 (49), 11205-11209.
  19. Dong, Y.; Wang, W.; Veiseh, O.; Appel, E. A.; Xue, K.; Webber, M. J.; Tang, B. C.; Yang, X.-W.; Weir, G. C.; Langer, R.; Anderson, D. G., Injectable and Glucose-Responsive Hydrogels Based on Boronic Acid-Glucose Complexation. *Langmuir* **2016**, 32 (34), 8743-8747.
  20. Figueiredo, T.; Jing, J.; Jeacomine, I.; Olsson, J.; Gerfaud, T.; Boiteau, J.-G.; Rome, C.; Harris, C.; Auzely-Velty, R., Injectable Self-Healing Hydrogels Based on Boronate Ester Formation between Hyaluronic Acid Partners Modified with Benzoxaborin Derivatives and Saccharides. *Biomacromolecules* **2019**, 21 (1), 203-239.
  21. Chen, Y.; Wang, W.; Wu, D.; Nagao, M.; Hall, D. G.; Thundat, T.; Narain, R., Injectable Self-Healing Zwitterionic Hydrogels Based on Dynamic Benzoxaborole-Sugar Interactions with Tunable Mechanical Properties. *Biomacromolecules* **2018**, 19 (2), 596-605.
  22. Wang, Y.; Li, L.; Kotsuchibashi, Y.; Vshyvenko, S.; Liu, Y.; Hall, D.; Zeng, H.; Narain, R., Self-Healing and Injectable Shear Thinning Hydrogels Based on Dynamic Oxaborole-Diol Covalent Cross-Linking. *ACS Biomater. Sci. Eng.* **2016**, 2 (12), 2315-2323.
  23. Adamczyk-Wozniak, A.; Borys, K. M.; Sporzynski, A., Recent Developments in the Chemistry and Biological Applications of Benzoxaboroles. *Chemical Reviews* **2015**, 115 (11), 5224-5247.
  24. Dowlut, M.; Hall, D. G., An Improved Class of Sugar-Binding Boronic Acids, Soluble and Capable of Complexing Glycosides in Neutral Water. *J. Am. Chem. Soc.* **2006**, 128 (13), 4226-4227.
  25. Cromwell, O. R.; Chung, J.; Guan, Z., Malleable and Self-Healing Covalent Polymer Networks through Tunable Dynamic Boronic Ester Bonds. *J. Am. Chem. Soc.* **2015**, 137 (20), 6492-6495.
  26. Yount, W. C.; Loveless, D. M.; Craig, S. L., Strong means slow: Dynamic contributions to the bulk mechanical properties of supramolecular networks. *Angew. Chem., Int. Ed.* **2005**, 44 (18), 2746-2748.
  27. Yount Wayne, C.; Loveless David, M.; Craig Stephen, L., Small-molecule dynamics and mechanisms underlying the macroscopic mechanical properties of coordinatively cross-linked polymer networks. *J Am Chem Soc* **2005**, 127 (41), 14488-96.
  28. Hemshekhar, M.; Thushara, R. M.; Chandranayaka, S.; Sherman, L. S.; Kemparaju, K.; Girish, K. S., Emerging roles of hyaluronic acid bioscaffolds in tissue engineering and regenerative medicine. *Int. J. Biol. Macromol.* **2016**, 86, 917-928.
  29. Tam, R. Y.; Smith, L. J.; Shoichet, M. S., Engineering Cellular Microenvironments with Photo- and Enzymatically Responsive Hydrogels: Toward Biomimetic 3D Cell Culture Models. *Acc. Chem. Res.* **2017**, 50 (4), 703-713.
  30. Berube, M.; Dowlut, M.; Hall, D. G., Benzoboroxoles as Efficient Glycopyranoside-Binding Agents in Physiological Conditions: Structure and Selectivity of Complex Formation. *J. Org. Chem.* **2008**, 73 (17), 6471-6479.
  31. Wu, X.; Li, Z.; Chen, X.-X.; Fossey, J. S.; James, T. D.; Jiang, Y.-B., Selective sensing of saccharides using simple boronic acids and their aggregates. *Chem. Soc. Rev.* **2013**, 42 (20), 8032-8048.
  32. Macosko, C. W., Rheology: Principles, Measurements, and Applications. *Rheology: Principles, Measurements, and Applications* **1994**, (Ed.; VCH Publishers: Weinheim, Germany).
  33. Hudson, R. E.; Holder, A. J.; Hawkins, K. M.; Williams, P. R.; Curtis, D. J., An enhanced rheometer inertia correction procedure (ERIC) for the study of gelling systems using combined motor-transducer rheometers. *Physics of Fluids* **2017**, 29 (12), 121602.
  34. Krieger, I. M., Bingham Award Lecture—1989: The role of instrument inertia in controlled-stress rheometers. *Journal of Rheology* **1990**, 34 (4), 471-483.
  35. Abraham, M. J.; Murtola, T.; Schulz, R.; Páll, S.; Smith, J. C.; Hess, B.; Lindahl, B. E., *SoftwareX* **2015**, 1, 19-25.
  36. Berendsen, H. J. C.; Postma, J. P.; van Gunsteren, W. F.; Hermans, J., *Intermolecular Forces, ed. B. Pullman, Springer, Netherlands* **1981**, 331-342.
  37. Schmid, N.; Eichenberger, A. P.; Choutko, A.; Riniker, S.; Winger, M.; Mark, A. E.; Gunsteren, W. F., Definition and testing of the GROMOS force-field versions 54A7 and 54B7. *Eur. Biophys. J.* **2011**, 40 (7), 843-856.

38. Bussi, G.; Donadio, D.; Parrinello, M., Canonical sampling through velocity rescaling. *J. Chem. Phys.* **2007**, *126* (1), 014101/1-014101/7.
39. Berendsen, H. J. C.; Postma, J. P. M.; Van Gunsteren, W. F.; DiNola, A.; Haak, J. R., Molecular dynamics with coupling to an external bath. *J. Chem. Phys.* **1984**, *81* (8), 3684-90.
40. Frisch, M. J.; Trucks, G. W.; Schlegel, H. B.; Scuseria, G. E.; Robb, M. A.; Cheeseman, J. R.; Scalmani, G.; Barone, V.; Mennucci, B.; Petersson, G. A.; Nakatsuji, H.; Caricato, M.; Li, X.; Hratchian, H. P.; Izmaylov, A. F.; Bloino, J.; Zheng, G.; Sonnenberg, J. L.; Hada, M.; Ehara, M.; Toyota, K.; Fukuda, R.; Hasegawa, J.; Ishida, M.; Nakajima, T.; Honda, Y.; Kitao, O.; Nakai, H.; Vreven, T.; Montgomery, J., J. A.; Peralta, J. E.; Ogliaro, F.; Bearpark, M.; Heyd, J. J.; Brothers, E.; Kudin, K. N.; Staroverov, V. N.; Kobayashi, R.; Normand, J.; Raghavachari, K.; Rendell, A.; Burant, J. C.; Iyengar, S. S.; Tomasi, J.; Cossi, M.; Rega, N.; Millam, J. M.; Klene, M.; Knox, J. E.; Cross, J. B.; Bakken, V.; Adamo, C.; Jaramillo, J.; Gomperts, R.; Stratmann, R. E.; Yazyev, O.; Austin, A. J.; Cammi, R.; Pomelli, C.; Ochterski, J. W.; Martin, R. L.; Morokuma, K.; Zakrzewski, V. G.; Voth, G. A.; Salvador, P.; Dannenberg, J. J.; Dapprich, S.; Daniels, A. D.; Farkas, Ö.; Foresman, J. B.; Ortiz, J. V.; Cioslowski, J.; Fox, D. J., *Gaussian 09, Revision D.01; Gaussian, Inc., Wallingford CT.* **2009**.
41. Zhao, Y.; Truhlar, D. G., The M06 suite of density functionals for main group thermochemistry, thermochemical kinetics, noncovalent interactions, excited states, and transition elements: two new functionals and systematic testing of four M06-class functionals and 12 other functionals. *Theor. Chem. Acc.* **2008**, *120* (1-3), 215-241.
42. Marenich, A. V.; Cramer, C. J.; Truhlar, D. G., Universal Solvation Model Based on Solute Electron Density and on a Continuum Model of the Solvent Defined by the Bulk Dielectric Constant and Atomic Surface Tensions. *J. Phys. Chem. B* **2009**, *113* (18), 6378-6396.
43. Del Vigo, E. A.; Marino, C.; Stortz, C. A., Exhaustive rotamer search of the 4C1 conformation of  $\alpha$ - and  $\beta$ -D-galactopyranose. *Carbohydr. Res.* **2017**, *448*, 136-147.
44. Sameera, W. M. C.; Pantazis, D. A., A Hierarchy of Methods for the Energetically Accurate Modeling of Isomerism in Monosaccharides. *J. Chem. Theory Comput.* **2012**, *8* (8), 2630-2645.
45. Mierzwa, G.; Gordon, A. J.; Latajka, Z.; Berski, S., On the multiple B-O bonding using the topological analysis of Electron Localisation Function (ELF). *Comput. Theor. Chem.* **2015**, *1053*, 130-141.
46. Springsteen, G.; Wang, B., A detailed examination of boronic acid-diol complexation. *Tetrahedron* **2002**, *58* (26), 5291-5300.
47. Ellis, G. A.; Palte, M. J.; Raines, R. T., Boronate-Mediated Biologic Delivery. *J. Am. Chem. Soc.* **2012**, *134* (8), 3631-3634.
48. Mahalingam, A.; Geonnotti, A. R.; Balzarini, J.; Kiser, P. F., Activity and Safety of Synthetic Lectins Based on Benzoboroxole-Functionalized Polymers for Inhibition of HIV Entry. *Mol. Pharmaceutics* **2011**, *8* (6), 2465-2475.
49. Angyal, S. J., The composition of reducing sugars in solution: current aspects. *Adv. Carbohydr. Chem. Biochem.* **1991**, *49*, 19-35.
50. Thordarson, P., Determining association constants from titration experiments in supramolecular chemistry. *Chem. Soc. Rev.* **2011**, *40* (3), 1305-1323.
51. Huang, C. Y., Determination of binding stoichiometry by the continuous variation method: the Job plot. *Methods Enzymol.* **1982**, *87* (Enzyme Kinet. Mech., Pt. C), 509-25.
52. Ulatowski, F.; Dabrowa, K.; Balakier, T.; Jurczak, J., Recognizing the Limited Applicability of Job Plots in Studying Host-Guest Interactions in Supramolecular Chemistry. *J. Org. Chem.* **2016**, *81* (5), 1746-1756.
53. Norrild, J. C.; Eggert, H., Boronic acids as fructose sensors. Structure determination of the complexes involved using <sup>1</sup>JCC coupling constants. *J. Chem. Soc., Perkin Trans. 2* **1996**, (12), 2583-2588.
54. Norrild, J. C.; Eggert, H., Evidence for Mono- and Bidentate Boronate Complexes of Glucose in the Furanose Form. Application of <sup>1</sup>J-C Coupling Constants as a Structural Probe. *J. Am. Chem. Soc.* **1995**, *117* (5), 1479-84.
55. Pettignano, A.; Grijalvo, S.; Haering, M.; Eritja, R.; Tanchoux, N.; Quignard, F.; Diaz Diaz, D., Boronic acid-modified alginate enables direct formation of injectable, self-healing and multistimuli-responsive hydrogels. *Chemical Communications* **2017**, *53* (23), 3350-3353.
56. Charlot, A.; Auzely-Velty, R., Novel Hyaluronic Acid Based Supramolecular Assemblies Stabilized by Multivalent Specific Interactions: Rheological Behavior in Aqueous Solution. *Macromolecules* **2007**, *40* (26), 9555-9563.
57. Leibler, L.; Rubinstein, M.; Colby, R. H., Dynamics of reversible networks. *Macromolecules* **1991**, *24* (16), 4701-7.
58. Rubinstein, M.; Semenov, A. N., Thermoreversible gelation in solutions of associating polymers: 2. Linear dynamics. *Macromolecules* **1998**, *31* (4), 1386-1397.
59. Rubinstein, M.; Semenov, A. N., Dynamics of Entangled Solutions of Associating Polymers. *Macromolecules* **2001**, *34* (4), 1058-1068.
60. Van Duin, M.; Peters, J. A.; Kieboom, A. P. G.; Van Bekkum, H., Studies on borate esters. II. Structure and stability of borate esters of polyhydroxycarboxylates and related polyols in aqueous alkaline media as studied by boron-11 NMR. *Tetrahedron* **1985**, *41* (16), 3411-21.
61. Sato, T.; Aoyagi, T.; Ebara, M.; Auzely-Velty, R., Catechol-modified hyaluronic acid: in situ-forming hydrogels by auto-oxidation of catechol or photo-oxidation using visible light. *Polymer Bulletin* **2017**, *74* (10), 4069-4085.
62. Liu, C. T.; Tomsho John, W.; Benkovic Stephen, J., The unique chemistry of benzoxaboroles: current and emerging applications in biotechnology and therapeutic treatments. *Bioorg Med Chem* **2014**, *22* (16), 4462-73.
63. Tomsho, J. W.; Pal, A.; Hall, D. G.; Benkovic, S. J., Ring Structure and Aromatic Substituent Effects on the pKa of the Benzoxaborole Pharmacophore. *ACS Med. Chem. Lett.* **2012**, *3* (1), 48-52.
64. Miyamoto, C.; Suzuki, K.; Iwatsuki, S.; Inamo, M.; Takagi, H. D.; Ishihara, K., Kinetic Evidence for High Reactivity of 3-Nitrophenylboronic Acid Compared to Its Conjugate Boronate Ion in Reactions with Ethylene and Propylene Glycols. *Inorg. Chem.* **2008**, *47* (5), 1417-1419.
65. Peters, J. A., Interactions between boric acid derivatives and saccharides in aqueous media: Structures and stabilities of resulting esters. *Coord. Chem. Rev.* **2014**, *268*, 1-22.
66. Hatakeyama, H.; Hatakeyama, T., Interaction between water and hydrophilic polymers. *Thermochim. Acta* **1998**, *308* (1-2), 3-22.
67. Haxaire, K.; Marechal, Y.; Milas, M.; Rinaudo, M., Hydration of hyaluronan polysaccharide observed by IR spectrometry. II. Definition and quantitative analysis of elementary hydration spectra and water uptake. *Biopolymers* **2003**, *72* (3), 149-161.

68. Joshi, H. N.; Topp, E. M., Hydration in hyaluronic acid and its esters using differential scanning calorimetry. *Int. J. Pharm.* **1992**, *80* (2-3), 213-25.
69. Servaty, R.; Schiller, J.; Binder, H.; Arnold, K., Hydration of polymeric components of cartilage - an infrared spectroscopic study on hyaluronic acid and chondroitin sulfate. *Int. J. Biol. Macromol.* **2001**, *28* (2), 121-127.